Influence of Fe on the room and high-temperature sliding wear of NiAl coatings

C. Brunetti [a,1,2], L.P. Belotti [b,2], M.H. Miyoshi [c,3], G. Pintaúde [d,4], A.S.C.M. D'Oliveira [a,*]

[a] Universidade Federal do Paraná, PG-MEC, Centro Politécnico, 81.531-990 Curitiba, PR, Brazil
[b] Universidade Federal do ParanáPR, CNPq, Centro Politécnico, 81.531-990 Curitiba, Brazil
[c] Universidade Tecnológica Federal do Paraná, CNPq 81.531-990 Curitiba, PR, Brazil
[d] Universidade Tecnológica Federal do Paraná, PPGEM, 80.230.901 Curitiba, PR, Brazil

ARTICLE INFO

ABSTRACT

High temperature mechanical properties of Ni–Al intermetallic alloys make them potential candidates as wear-resistance materials or coatings to protect components operating in harsh environments. In-situ processing of Ni–Al intermetallic coatings has been successfully carried out previously. The role of interaction with the substrate, measured by the Fe content in NiAl coatings, on the wear performance is addressed in this study. Mixtures of Ni and Al powders were prepared (65 at.%Ni-35 at.%Al) and deposited onto 1020 steel disks. Three deposition current were used (100, 120 and 150 A) resulting in coatings with Fe content ranging from 36 to 50 at.%, as a consequence of the metallurgical bond with the substrate steel. The development of the NiAl was confirmed by X-ray diffraction together with austenite. Dry sliding tests were carried out at room temperature and 710 °C, using a ball-on-disk tribometer with a 3.0 mm Al_2O_3 ball under different normal loads (1, 3 and 5 N). Temperature played an important role on the wear behavior and the wear coefficient was reduced by one order of magnitude at 710 °C. At room temperature, wear coefficients increased with the applied load, and abrasion was the main observed mechanism regardless of the iron content in coatings. However, at 710 °C the variations on the wear coefficient cannot be associated with the coating hardness and wear was dominated by oxidation. Hematite was identified on all the oxidized surfaces. Notwithstanding, for the coatings with higher Fe content the continuous and thicker scale accounts for the measured stable wear coefficient regardless of the applied load.

© 2014 Elsevier B.V. All rights reserved.

1. Introduction

Plasma transferred arc (PTA) is a versatile process regarding its ability to tailor wear-resistant coatings. Depositing alloys have been modified with alloying elements that form self-lubricant constituents [1] to improve the sliding wear performance, hard second phases [2] that increase the abrasion resistance or aluminides to improve carburization resistance [3]. The final chemical composition of coatings is also affected by the substrate because of the metallurgical bond with the deposited material.

High-temperature wear requires specific alloy design, to guarantee the stability of the mechanical properties [4], and to control oxidation resistance [5], both playing an important role on the performance of the surface. Intermetallic alloys, in particular aluminide alloys, are attractive materials for high temperature applications. Their ordered structure offers stable mechanical behavior and Al_2O_3 oxide layer protection against oxidation.

Protecting iron based components with aluminide coatings leads to enhanced performance under harsh environments, particularly under elevated temperature. Although a few studies in the literature refer to the evaluation of NiAl cast alloys, the understanding of the behavior of coatings requires further studying. In-situ synthesis of the aluminide by PTA [6] showed that the interaction with the steel substrate resulted in a high Fe content, up to 60%. However, the impact on properties and performance of coatings is yet to be addressed.

The effect of Fe content on oxidation resistance and on sliding wear of Ni–Al containing different amounts of Fe has been addressed individually. Monteiro et al. [7] analyzed Ni–Al alloys with iron content ranging from 20 to 30 at.%. The sliding wear of the aluminide compounds containing different amounts of Fe was investigated by Munroe et al. [8], but the oxidation did not play an important role in their experimental setup. The tribological behavior of Ni–Al alloys containing large fractions of iron and its role when tribochemical reactions occur require

* Corresponding author at: Mechanial Engineering Deparment, Universidade Federal do Paraná, Centro Politécnico, 851990, Curitiba/PR, Brazil. Tel.: + 554133613119.
E-mail addresses: sofmat@ufpr.br (C. Brunetti), pintaude@utfpr.edu.br (G. Pintaúde).
[1] Presently at IFPR, Paranaguá/PR, Brazil.
[2] Tel.:+55 41 3361 3119.
[3] Tel.: + 55 41 3310 4852.
[4] Tel./fax: + 55 41 3310 4499.

Table 1
PTA deposition parameters.

Variable	Unit	Value
Plasma gas flow (Ar)	(l min^{-1})	2.0
Shield gas flow (Ar)		15.0
Carrier gas flow (Ar)		1.0
Powder feed rate	(g min^{-1})	5.8
Torch stand off	(mm)	10.0
Travel speed	(mm min^{-1})	100.0

Table 2
Sliding wear tests parameters.

Test conditions	unit	Specification
Counter body material	Ball	Al$_2$O$_3$
Diameter	mm	Ø 3
Applied force	N	1, 3 and 5
Velocity	m s^{-1}	0.25
Sliding distance	m	750
Temperature	°C	27 or 710
Relative humidity	%	58–62

specific studies that can complement the understanding of Ni–Al hardfacing coatings.

The present study addresses the consequences of Fe content on the wear performance of Ni–Al coatings. The hypothesis is that the properties of the Ni–Al compounds depend on the Fe content and that the oxide layer that forms on these alloys plays a determining role on the wear process at relatively small loads.

2. Materials and methods

Powder mixtures of elemental nickel and aluminum (65 at.%Ni–35 at.%Al) were homogenized for 1 h at 80 rpm in a Y mixer and dried at 70 °C for 24 h. The synthesis of coatings occurred during deposition by Plasma Transferred Arc on an AISI 1020 steel substrate (Ø55 mm × 20 mm). This steel was selected to guarantee that Fe was the main element from the substrate participating in the aluminide coating. The substrates were pre-heated at 200 °C before deposition to minimize cracking susceptibility. In-situ synthesis of the aluminides was carried out with three deposition current (100, 120 and 150 A) all other parameters were kept constant, Table 1. Circular tracks were deposited in order to meet the wear set up requirements, Fig. 1 shows a schematic representation of sample geometry.

The transverse cross sections of the single-track coatings were prepared using standard metallographic procedures. Specimens were electrolitically etched in a 50 ml HCl, 50 ml H$_2$O (distilled) and 10 g CuSO$_4$ solution and the microstructure was investigated using laser confocal (LCM) and scanning electron microscopy (SEM). The semi-
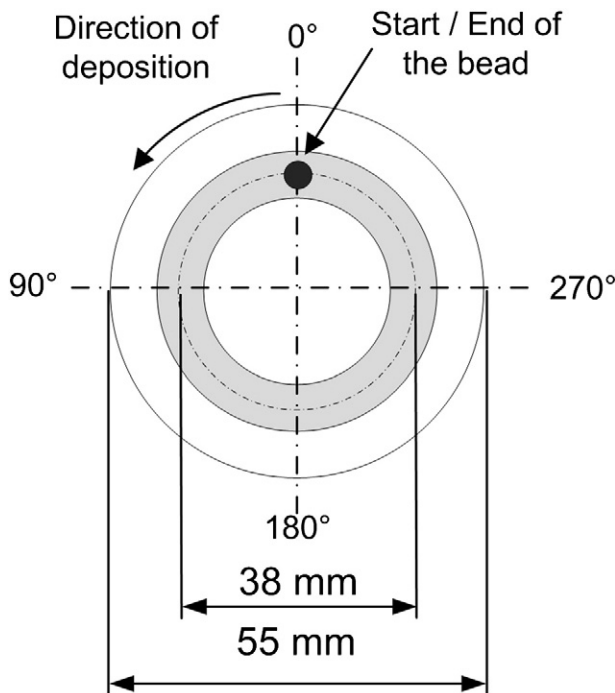
quantitative chemical analyses were carried out on a 200 × 200 μm^2 area by energy dispersive spectroscopy (EDS).

The X-ray diffraction analysis (XRD) on a polished top surface of samples extracted from the coatings (20 × 20 mm^2) used Cu Kα radiation (λ = 0.15406 nm). During the analysis specimens were stationary. The equipment was adjusted to operate in continuous mode scan with 0.50°·min^{-1} scan speed and sampling pitch of 0.02°.

The microhardness was measured from the load–displacement curve produced by a Vickers indenter, according to the ISO/FDIS 14577-1 [9] standard recommendations. Profiles under a load of 3 N were determined for each coating as an average of a minimum of three profiles.

Surface preparation for the wear tests includes grinding a 0.5 mm thick layer followed by metallographic procedures to achieve a surface finishing of a 1 μm diamond polish. This surface finishing procedure guarantees that specimens attended the specifications of the ASTM G-99 wear testing standard [10].

Sliding wear tests were performed in a High Temperature tribometer, using a ball-on-disk configuration, with an alumina ball sliding against the Ni–Al coatings. Testing conditions were selected to guarantee that a) no significant ball wear occurs, and b) after 200 m, stationary wear as a function of sliding distance, in agreement with the experimental set up of Sierra and Vasquez [11]. The tests were carried out at room temperature and at 710 °C, under applied load of 1, 3 and 5 N, respectively. The sliding distance and the velocity were kept constant for all test conditions, and the relative humidity was kept within the 58–62% range. Table 2 summarizes the wear test conditions.

Worn track geometry was measured by perfilometry using laser confocal microscopy. Analysis considered the four quadrants of the circular single-track coatings (Fig. 1) to determine the worn area, A_{ST}. Values were averaged over at least thirty (30) measurements per sample, and were used to calculate the total wear volume, Eq. (1):

$$Q = A_{ST} * P \tag{1}$$

Fig. 1. Schematic representation of deposited circular Ni–Al single-track coatings.
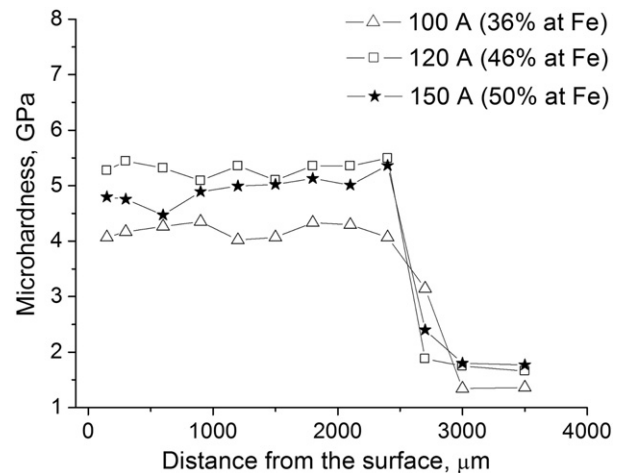

Fig. 2. Microhardness profiles of coatings processed with the Ni–Al powder mixtures on AISI 1020 substrate with different deposition current.
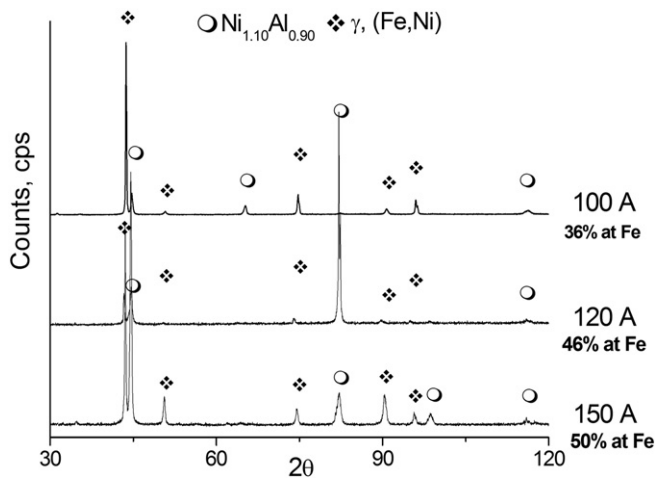
Fig. 3. XRD patterns at the top surface of coatings processed with the Ni–Al powder mixtures with different deposition current.

Fig. 5. Wear coefficient variation with the applied load at room temperature for the Ni–Al coatings with different iron contents.

where, A_{ST} = average worn area, measured in cross-section (mm²)P = perimeter of worn track (mm).

The wear results are presented using the dimensional wear coefficient, k, defined by Eq. (2)

$$\kappa = \frac{Q}{l \cdot W} \qquad (2)$$

where, Q = wear volume (mm³)l = sliding distance (m)W = applied load (N).

To individually assess the effect of temperature on the processed Ni–Al coatings samples were heat treated in an air furnace at 710 °C for 1 h and air-cooled. The characterization of the oxides at the surface of coatings was carried out by Raman Spectroscopy using an Ar ion laser (532 nm).
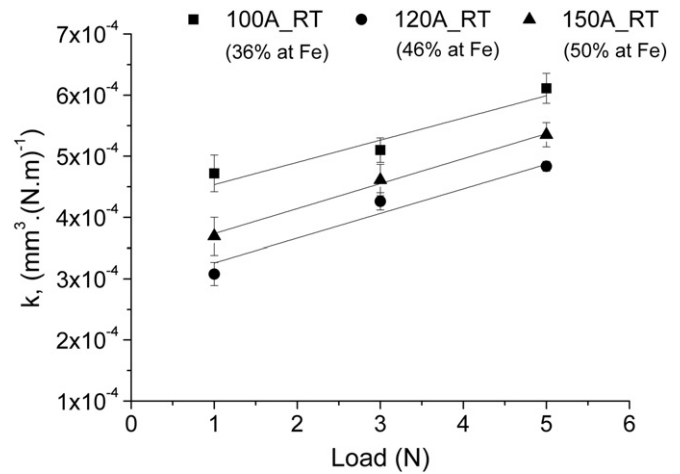
3. Results and discussion

3.1. As-deposited coatings

The influence of the deposition current (iron content) on the characteristics of the coatings processed with the Ni + 35 at.%Al powder mixture was first assessed by the microhardness profiles, Fig. 2.

A stable hardness profile along the transverse cross section of the 2500 μm thick coatings is observed regardless of the deposition current. In spite of the increase on the Fe content in the NiAl coatings with deposition current the subsequent decrease on coating hardness exhibited by superalloy coatings [12] was not observed. The harder coating was that processed with 120 A, the intermediate current tested, suggesting that the synthesis that occurred during deposition might have a role on this behavior. Phase analysis by XRD contributed to better understand this behavior, Fig. 3. The formation of dual phase coatings
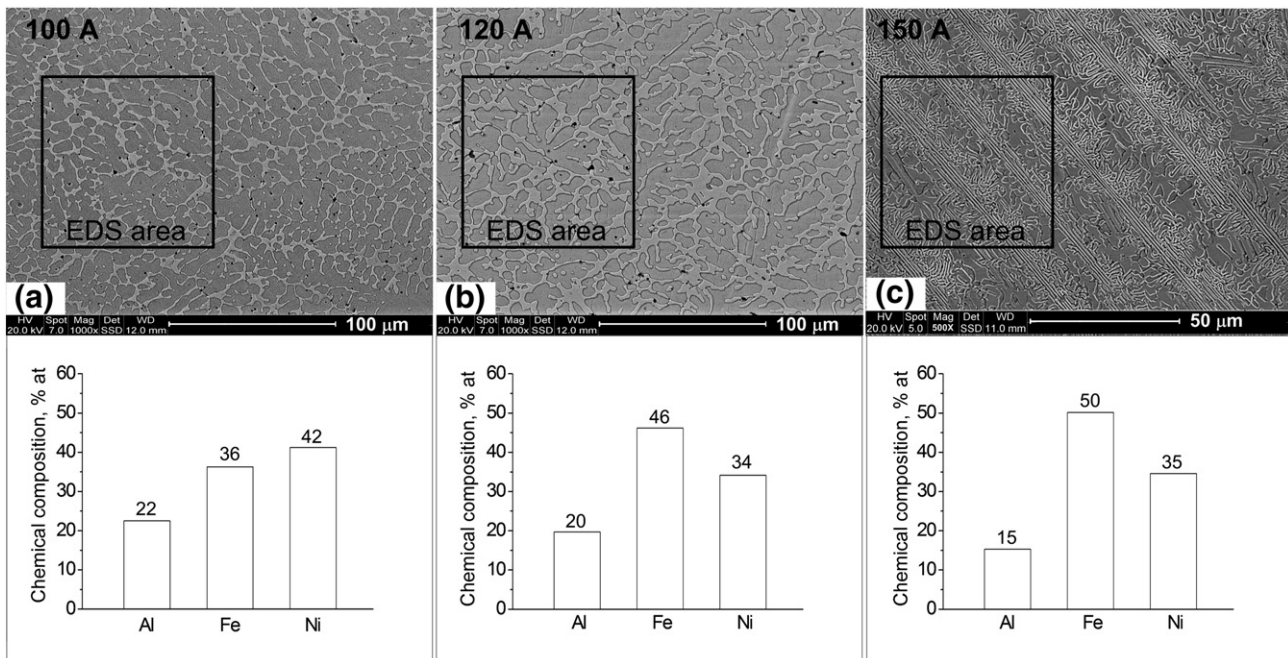

Fig. 4. Microstructure observed at the transverse cross-section of coatings and 200 × 200μm² EDS analysis, (a) deposition with 100 A, (b) deposition with 120 A and (c) deposition with 150 A.

constitute by an austenite (Fe, Ni) solid solution and the ordered aluminide NiAl. The later confirming the synthesis of the aluminide during the PTA deposition of the powder mixture, in agreement with previous results [6].

XRD results showed that a fraction of austenite was always identified. However, the coating processed with 120 A has the lowest fraction of austenite, given by the peak intensity, accounting for the higher hardness measured. A solidification texture was formed in this coating confirmed by the higher intensity peak for the $Ni_{1.1}Al_{0.9}$ compound identified at a higher 2θ. The increase in the iron content in this ordered compound and consequent lattice distortion is denoted by the wider peaks in the 150 A coatings.

Fig. 4 presents the microstructures of processed coatings and chemical analysis by EDS. A dendritic solidification structure can be observed. Semi-quantitative chemical analysis by EDS showed an increase on the Fe content in coatings as the deposition current increased. This is a consequence of the interaction with the substrate. The Fe content in coatings was measured: 36, 46 and 50 at.% for 100, 120 e 150 A, respectively.

Previous results on the analysis of linear single track Ni–Al coatings [13] revealed that the coating hardness increased linearly with the Fe content, which was associated with the distribution of the Fe atoms in the lattice of NiAl intermetallic compound, in agreement with models described in the literature [14,15]. However, for the 38 mm diameter circular single track coating hardness does not exhibit a linear correlation with the Fe content in coatings. Although coatings were processed on the same substrate steel, deposition as a linear or circular single-track coating affects cooling rate differently as the heat flow follows the torch travel speed and deposition path. The former allows for the coatings to cool as the torch moves away from the melt pool whereas in the circular path the torch returns to its initial position compromising the cooling rate. For the lower deposition current tested the effect is less intense and so is the interaction with the substrate, measured by the Fe content in coatings. According to the Ni–Al–Fe phase diagram the amount of austenite formed varies with the Fe content in agreement with the X-ray results.

3.2. Wear performance

Assessing wear behavior at room temperature and at 710 °C revealed significant differences on the behavior of coatings associated with the features of the phenomena occurring at the surface for each condition.

The dimensional wear coefficient exhibited a linear relationship with the applied load for tests performed at room temperature, Fig. 5, which can be associated with a single wear mechanism during the steady-state regime of wear [16].

Analysis of the worn tracks, Fig. 6, suggests the formation of third-body particles, accounting for the observed scoring and grooving. The presence of third-body particles in sliding systems is a common occurrence [17,18] and is associated with the detachment of material from the surfaces in contact during sliding. The characterization of the worn surface of coatings and that of the alumina sphere (Fig. 7a and b)
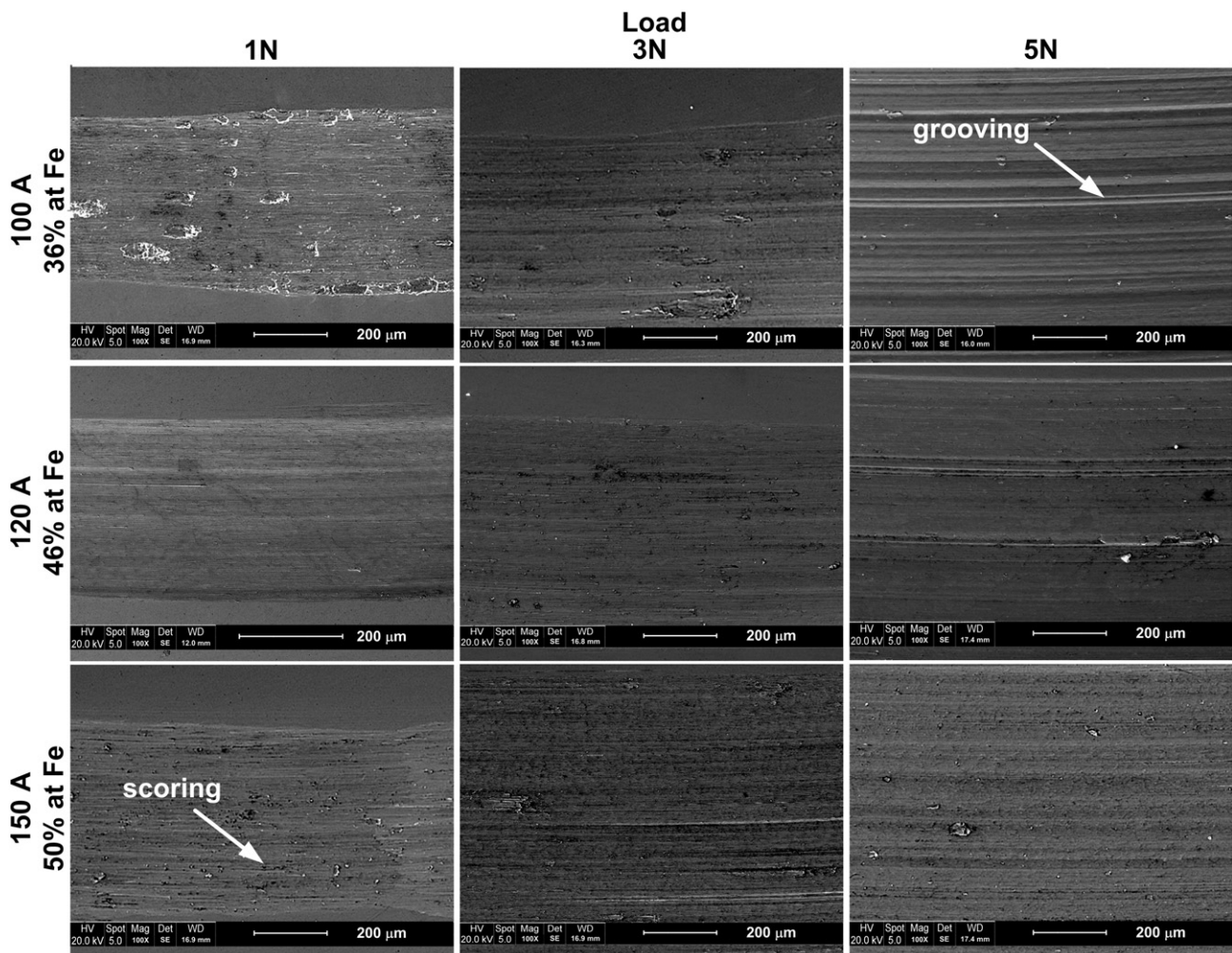

Fig. 6. Worn surface morphologies tested at room temperature with different normal loads.
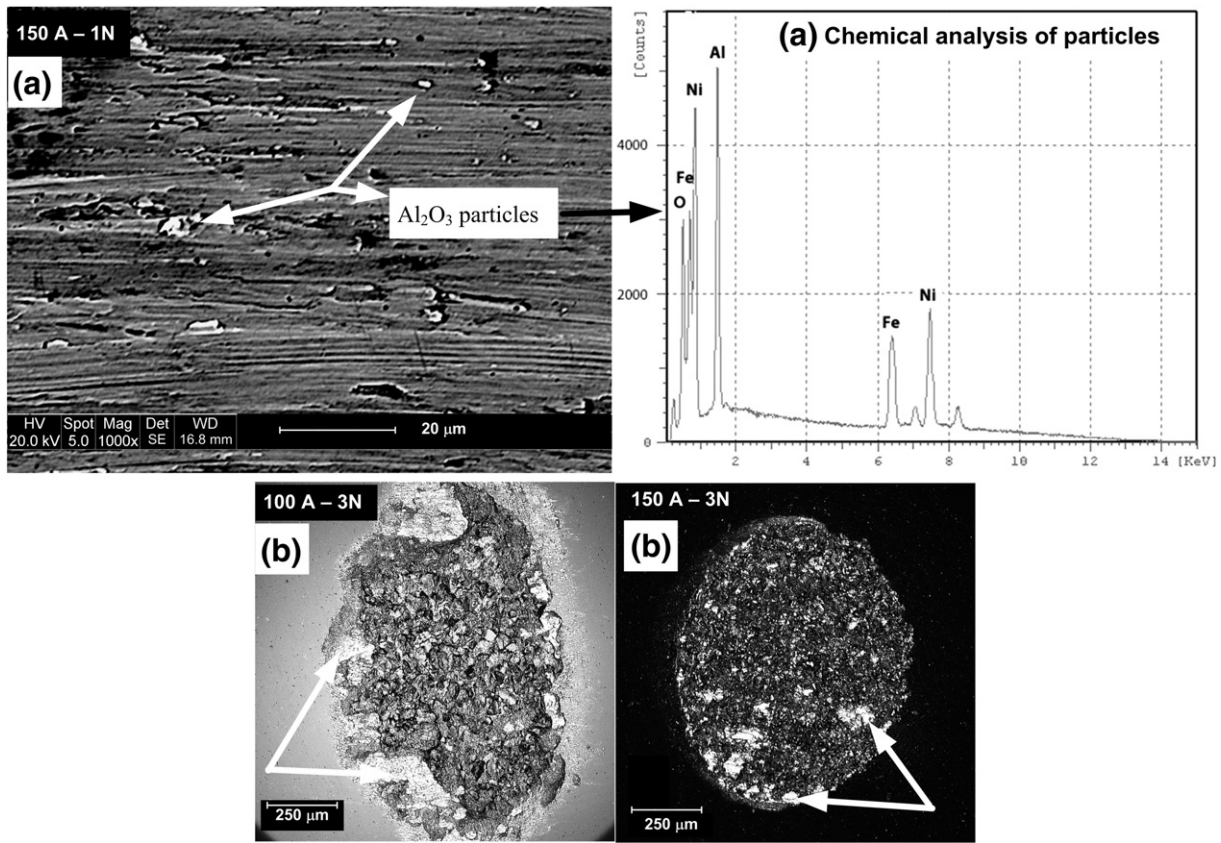
Fig. 7. (a) Al_2O_3 particles adhered on surface as result of wear of the alumina ball (white arrows); (b) adhered material on the alumina ball surface after testing Ni–Al coatings with 36 at.%Fe (100 A) and 50 at.%Fe (150 A).

confirmed the detachment of material. Alumina particles on the coating surface and adhered material on the alumina sphere are observed and probably occurred during the running-in stage.

A different scenario is presented after high temperature wear tests and the linear relationship between applied load and the wear coefficient exhibited at room temperature does not describe the high-temperature behavior, (Fig. 8), particularly for the richer Fe coatings. As a general observation the wear resistance is better under high temperature but significant differences between coatings were measured. Lower wear coefficient values, k, were determined from tests carried out at 710 °C. Two different responses to the applied load during wear tests can be established on coatings processed with 100 A and 150 A, respectively.
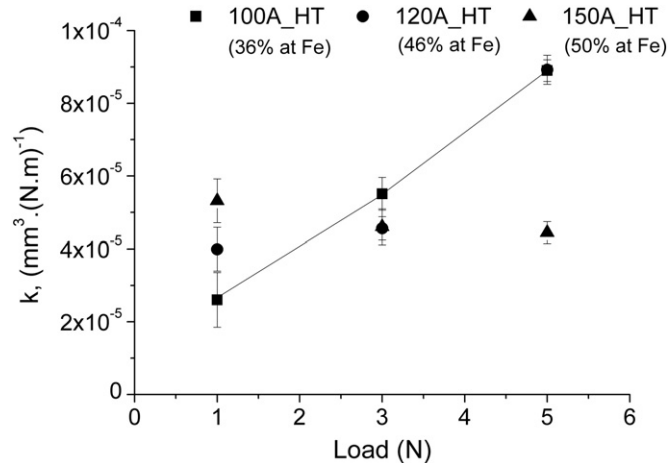
The former showed an increase on k with the applied load, similar behavior to that observed at room temperature. Coatings processed with the higher deposition current, 150 A, exhibited a stable wear coefficient, k, regardless of the applied load. A strong dependence on the applied load was shown by coatings processed with 120 A, up to 3 N a stable k was determined whereas under an applied load of 5 N the wear coefficient increased.

Analysis of the cross-section of worn coatings and following exposure to temperature contributed to the understanding of the role of formed scales on the wear behavior, Figs. 9 and 10. A continuous iron oxide layer is observed in the wear track. Isothermal oxidation tests showed the formation of the oxide layer to vary depending on the
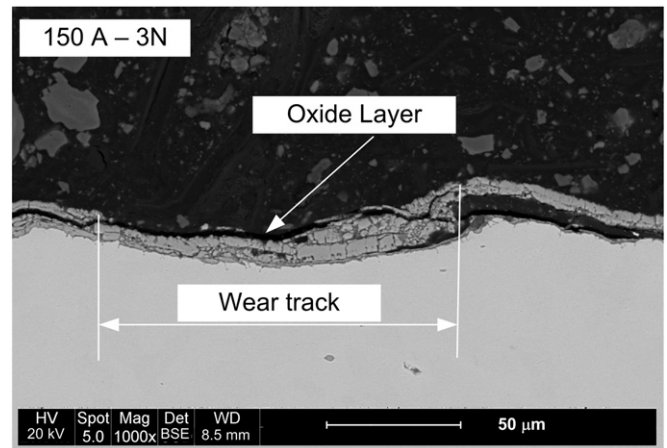

Fig. 8. Wear coefficient variation with the applied load at 710 °C for the Ni–Al coatings with different iron contents.

Fig. 9. Cross section of the as-deposited coating processed with 150 A after wear testing at 710 °C under 3 N load. The continuous Fe oxide layer on the wear track is observed.
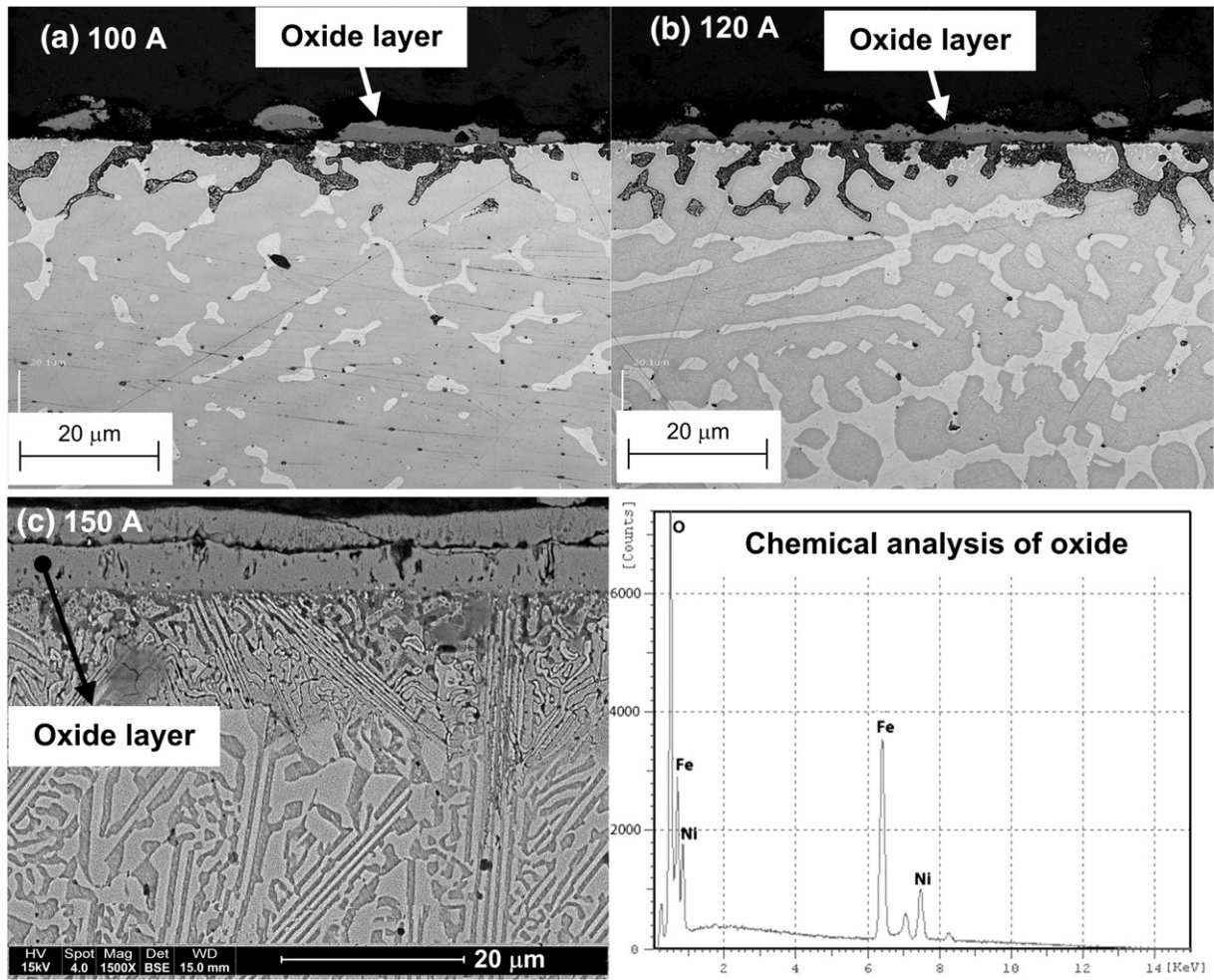
Fig. 10. Cross sections of coatings exposed at 710 °C for 1 h. In an air furnace a) deposition with 100 A (36 at.%Fe), BSE image, no etching, b) deposition with 120 A (46 at.%Fe), BSE image, no etching and c) deposition with 150 A (50 at.%Fe), SE after etching and corresponding EDS of the oxide layer.

deposition current and as a consequence on the iron content of coatings. On coatings processed with the lower deposition current tested the oxidation of the interdendritic regions and a few particles of oxide at the surface the can be identified, Fig. 10a. Increasing the amount of Fe in coatings increased oxidation in the interdendritic regions and an oxide layer that better wets the surface is observed, Fig. 10b. Fig. 10c
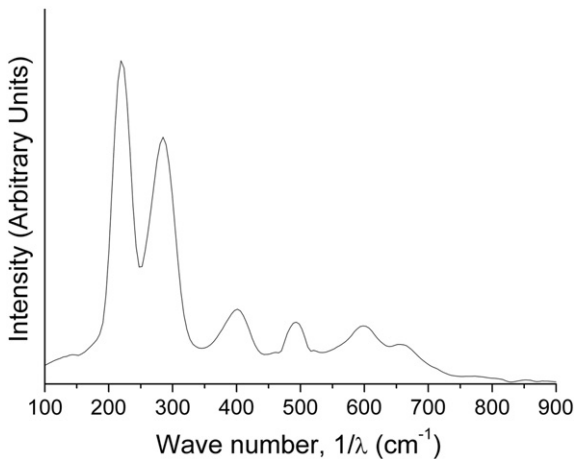

Fig. 11. Raman spectroscopy (laser with λ 532 nm) for coating processed under 150 A after thermal exposure at 710 °C for 1 h, showing the Fe oxide spectrum.

shows a thicker and continuous oxide layer on coatings processed with 150 A. The EDS analysis agrees with that of worn surfaces and shows peaks for the iron, suggesting the migration of Fe atoms for the surface to form an iron oxide. Raman spectroscopy analysis within the range for hematite (Fe_2O_3) [19] and alumina (3000–5500 cm^{-1}) [20] was carried out and confirmed that only the iron oxide was formed at the surface of coatings processed with 150 A, Fig. 11. The relative position of peaks is shown in Table 3, together with the literature data for this phase.

The kinetics of oxidation of the different elements at the surface and the furnace temperature will determine the oxide that forms at the surface of coatings. Although alumina is thermodynamically more stable the larger amount of Fe and faster growth of the iron oxide determined its formation.

The oxide at the surface of coatings affected the worn surfaces of Ni–Al coatings processed at 710 °C, as shown in Fig. 12. Analysis of the high temperature worn surfaces confirms that an abrasive agent is present particularly on the surface of coatings processed with 100 A and 120 A. Worn track exhibits scoring and grooving evidences of the

Table 3
Identification of peaks position of hematite within Raman spectra.

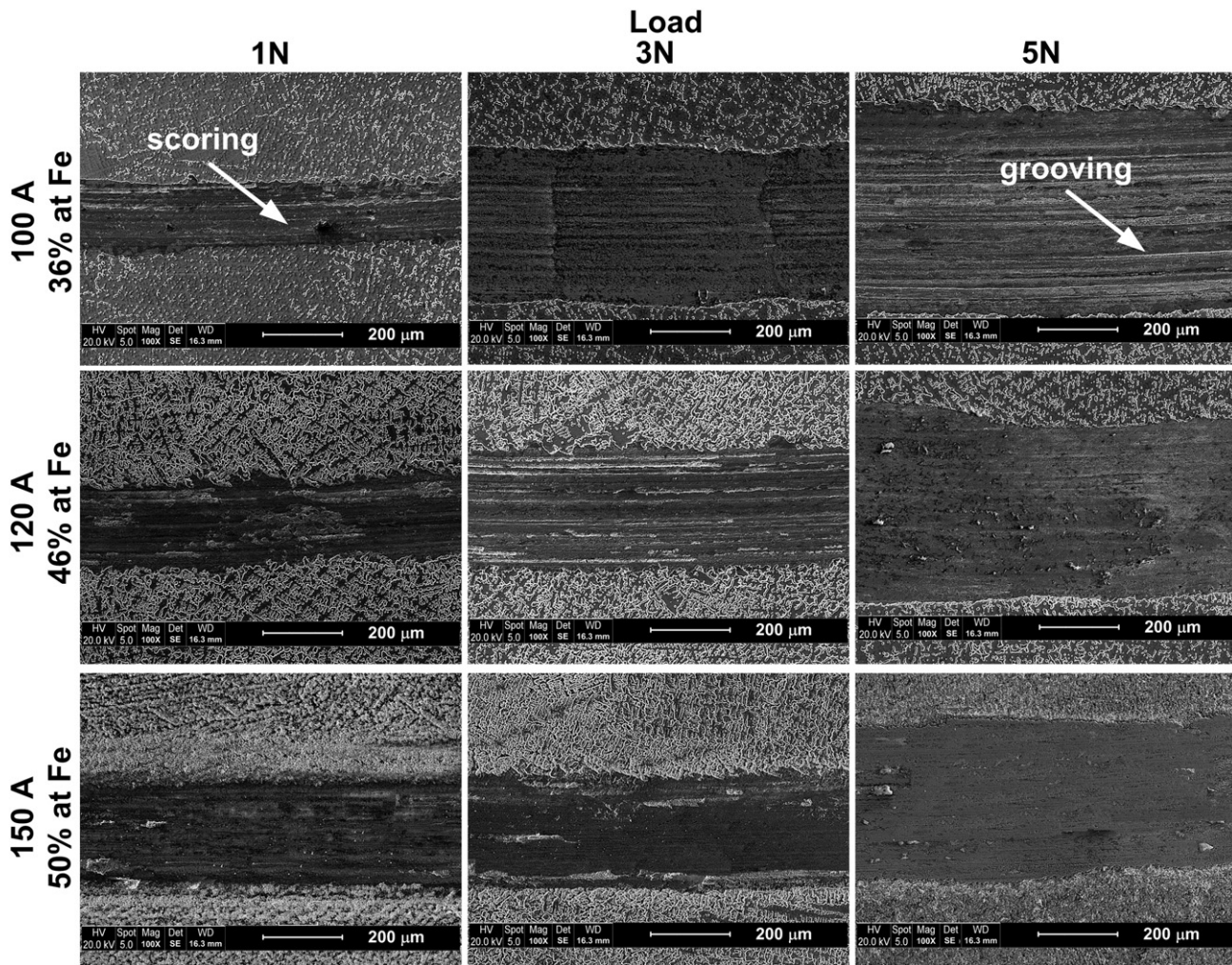|	Position of hematite peaks within Raman spectra (cm^{-1})					
Fig. 10	222	287	404	491	600	658
Chico et al., (2011) [20]	227	293	409	498	611	658

Fig. 12. Worn surface morphologies tested with different normal loads at 710 °C.

abrasion mechanism, which contributed to an increase of the wear rates. Fracture of the oxide layer, Fig. 13, spallation or the detachment of the discontinuous thin oxide at the surface accounts for the increase on the wear coefficient, k, with the applied load.

A constant wear coefficient, k, regardless of the applied load reveals the different behaviors of coatings processed with 150 A, which contain the higher measured Fe content. The worn surfaces did not exhibit neither scoring nor grooving, confirming the less significant role of third body formation on this coating. The continuous hematite layer and its hardness can account for the measured wear behavior with increasing applied load. The maintenance of the oxide layer, or even its fast renewal, during a sliding wear process reduces considerably the wear rate of the system. At 710 °C, the combination between the properties of the iron oxide and those of coating processed under
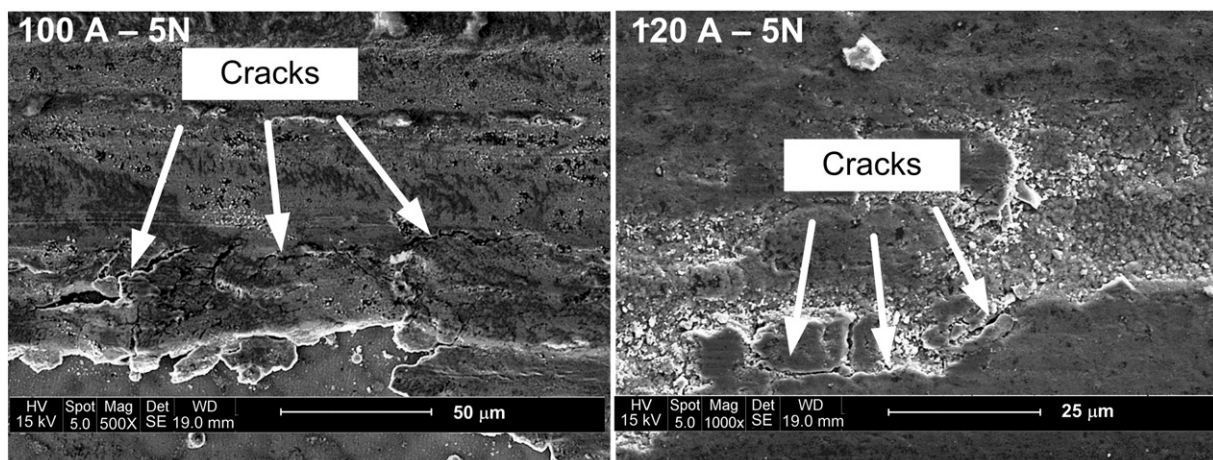

Fig. 13. Cracks (arrows) observed on surface scales on coatings processed with 100 A and 120 A, respectively, after wear tests at 710 °C under an applied load of 5 N.

150 A exhibited a compatibility that results in a beneficial effect for the wear system.

4. Conclusions

Ni–Al intermetallic coatings were processed during the PTA deposition of mixtures of Ni and Al powders using three deposition currents to obtain different Fe contents. Ball-on-disk sliding wear tests conducted at room and high-temperatures, allowed concluding:

1. At room temperature Ni–Al coating wear coefficient, k, increased linearly with the applied load as a consequence of the adhered particles on both ball and disk making the effects of abrasion mechanisms dominate during the wear.
2. At 710 °C the iron content in coatings resulted in the formation of hematite with different features, the harder and discontinuous layer on coatings processed with 100 A and 120 A accounts for the predominance of abrasive wear mechanisms and the increase of the wear coefficient with the applied load. However, for the richer iron coatings the continuous hematite layer and the better compatibility with the Ni–Al–Fe coatings resulted in a change on the wear behavior confirmed by the constant wear coefficient, k, regardless of the applied load.

Acknowledgments

References

[1] P. Skarvelis, G.D. Papadimitriou, M. Perraki, J. Tribol. (Trans. ASME) 132 (2010) 03130.
[2] Y.F. Liu, X.-B. Liu, X.-Y. Xu, S.-Z. Yang, Surf. Coat. Technol. 205 (2010) 814–819.
[3] F.J.R. Cangue, A.S.C.M. D'Oliveira, Mater. Chem. Phys. 120 (2010) 552–557.
[4] H. Berns, A. Fischer, Wear 162–164 (PART A) (1993) 441–449.
[5] F.H. Stott, Tribol. Int. 35 (2002) 489–495.
[6] V.B. Almeida, E.H. Takano, I. Mazzaro, A.S.C.M. D'Oliveira, Surf. Eng. 27 (2011) 266–271.
[7] F.R. Assuncao, Z. Chaoliu, M. de J. Monteiro, Mater. Res. 2 (1999) 181–184.
[8] P.R. Munroe, M. George, I. Baker, F.E. Kennedy, Mater. Sci. Eng. A 325 (2002) 1–8.
[9] International Organization for Standardization, ISO/FDIS 14577-1 metallic materials — instrumented indention test for hardness and materials parameters, 2002. 25.
[10] American Society for Testing Materials — ASTM, G99: Standard Test Method for Wear Testing with a Pin-on-Disk Apparatus, ASTM International, West Conshohocken, PA, 2005.
[11] C. Sierra, A.J. Vázquez, Intermetallics 14 (2006) 848–852.
[12] A.E. Yaedu, A.S.C.M. D'Oliveira, Mater. Sci. Technol. 21 (2005) 459–466.
[13] C. Brunetti, G. Pintaude, A. S. C. M. D'Oliveira, The Influence of Fe Content on the Mechanical Properties of NiAl Coatings Processed In-Situ, J. of Mater. Eng and Perform., DOI: http://dx.doi.org/10.1007/s11665-014-1203-5.
[14] I.M. Anderson, A.J. Duncan, J. Bentley, Intermetallics 7 (1999) 1017–1024.
[15] L.M. Pike, Y.A. Chang, C.T. Liu, Intermetallics 5 (1997) 601–608.
[16] E. Rabinowicz, Int. Lubrication Conf., San Francisco, California, American Soc. Mech. Eng. and Am. Soc. Lubrication Eng., 1980, (6 pp.).
[17] I.A. Inman, P.K. Datta, H.L. Du, J.S. Burnell-Gray, S. Pierzgalski, Q. Luo, Tribol. Int. 38 (2005) 812–823.
[18] J. Jiang, F.H. Stott, M.M. Stack, Tribol. Int. 31 (1998) 245–256.
[19] D. Chicot, J. Mendoza, A. Zaoui, G. Louis, V. Lepingle, F. Roudet, J. Lesage, Mater. Chem. Phys. 129 (2011) 862–870.
[20] V.K. Tolpygo, D.R. Clarke, Mater High Temp 17 (2000) 59–70.